



High benthic methane flux in low sulfate oceans: Evidence from carbon isotopes in Late Cretaceous Antarctic bivalves

Joanna L.O. Hall^{a,*}, Robert J. Newton^a, James D. Witts^{a,1}, Jane E. Francis^b,
Stephen J. Hunter^a, Robert A. Jamieson^a, Elizabeth M. Harper^c, J. Alistair Crame^b,
Alan M. Haywood^a

^a School of Earth and Environment, University of Leeds, West Yorkshire, LS2 9JT, United Kingdom

^b British Antarctic Survey, Madingley Road, Cambridge, CB3 0ET, United Kingdom

^c Department of Earth Sciences, University of Cambridge, Downing Site, Cambridge, CB2 3EQ, United Kingdom

ARTICLE INFO

Article history:

Received 24 March 2017

Received in revised form 23 May 2018

Accepted 10 June 2018

Available online 20 June 2018

Editor: H. Stoll

Keywords:

Seymour Island
Antarctica
stable isotopes
seasonal
carbon cycle
methane

ABSTRACT

The shell material of marine benthic bivalves provides a sensitive archive of water chemistry immediately above the sediment–water interface, which in turn is affected by sedimentary geochemistry and redox reactions. Sulfate has a major controlling effect on sedimentary carbon cycling, particularly the processes of methane production and oxidation, with lower concentrations of sulfate likely resulting in an increase in sedimentary methane production. Whilst it is accepted that ocean sulfate varied markedly across the Phanerozoic, evidence of changes in methane production in sediments has so far been lacking. There is potential for the oxidation products of sedimentary methane to be preserved and detected in marine fossils. Here we present the results of high resolution carbonate isotope records from two taxa of well-preserved shallow-infaunal bivalve (*Lahillia* and *Cucullaea*) collected from the marine shelf succession across the Cretaceous–Paleogene (K–Pg) boundary in Seymour Island, Antarctica. The succession has pre-existing subtle indications of more abundant methane, and the time period is characterized by much lower marine sulfate concentrations than modern.

These shell carbonate–carbon isotope records vary widely: at one extreme, shells have typical average values and small ranges compatible with a contemporaneous marine dissolved inorganic carbon (DIC) source and modern-style sedimentary carbon cycling. At the other, the shells have large-amplitude annual cycles of carbon isotopic variability of up to 23.8‰ within a single year of growth and shell carbonate $\delta^{13}\text{C}$ compositions as negative as -34‰ . Shells with these increased ranges and unusually negative values are found at discrete intervals and across both bivalve taxa. The contribution of methane required to explain the most negative carbonate–carbon isotopic values in the bivalve shells is extremely high (between 30 to 85% of bottom-water DIC based on mass balance calculations). Records of organic–carbon isotopes from the same succession remained between -26.1 and -21.7‰ throughout, suggesting that methane influence was restricted to bottom-waters. A lack of authigenic carbonate in the section indicates that methane oxidation progressed aerobically and may have provided a significant driver for transient bottom water de-oxygenation.

Where methane addition is indicated, the seasonal sensitivity precludes control by methane hydrates. We argue that these data represent the increased importance and sensitivity of methanogenesis in the sediments, enabled by lower ocean sulfate concentrations during the Late Cretaceous. The tendency towards a more dynamic role for marine methane production and oxidation is likely to apply to other times of low marine sulfate in Earth's history.

© 2018 The Authors. Published by Elsevier B.V. This is an open access article under the CC BY license (<http://creativecommons.org/licenses/by/4.0/>).

1. Introduction

Marine bivalves can be sensitive recorders of past bottom-water redox reactions, which are themselves conditioned by major seawater chemistry. In particular, records of marine dissolved inorganic carbon (DIC) can be preserved in the fossil record by

* Corresponding author.

E-mail address: eejlh@leeds.ac.uk (J.L.O. Hall).

¹ Present address: American Museum of Natural History, Central Park West at 79th Street, New York, NY, 10024.

biomineralizing organisms which incorporate carbon from the ambient DIC pool into biological compounds such as shell carbonate (McConnaughey and Gillikin, 2008). High resolution carbon isotope analysis was performed on specimens of Late Cretaceous and early Paleocene infaunal bivalves from a marine shelf succession cropping out on Seymour Island, Antarctica. This analysis was undertaken to examine variation in the composition of the marine DIC pool within lifetime growth cycles. In turn, this provides the potential for insight into changes in past productivity and redox conditions including methane oxidation.

The shells of infaunal bivalves are ideal archives in which to search for signals of methane oxidation in the benthic boundary layer of the water column. The active pumping of water by bivalves to supply food particles, oxygen, and ions for biomineralization means that the isotope signatures produced in modern shells are dominated by bottom water rather than sedimentary pore-water signatures (Klein et al., 1996). Some species do incorporate a small amount of respired organic carbon into their shell carbonate; however, most is precipitated from the DIC in inhaled seawater with little carbon isotope fractionation (McConnaughey et al., 1997; Poulain et al., 2010).

Examples of the infaunal genera *Lahillia* and *Cucullaea* were chosen for this study due to their abundance in the Seymour Island study section. Many specimens were collected in an intact or near-intact condition, and their large aragonitic shells and prominent internal or external shell growth lines make them ideal for high resolution geochemical studies. The visible growth lines were used to identify the cyclicity of shell growth; many species of bivalve produce these lines with distinct periodicity (i.e. annual, monthly, daily; Schöne et al., 2005b; Immenhauser et al., 2016). Each growth line represents a pause in the shell accretion, and the growth increment between consecutive lines records a period of active shell growth that can be used to identify the relative timing of geochemical signals incorporated into shell material from the ambient water. The large shell size (typically up to 10 cm in length) enabled microsampling for stable carbon and oxygen isotopic analysis within growth increments. A similar method was used by Buick and Ivany (2004) to analyze material from Eocene *Cucullaea raea* from Seymour Island and determine that shell production occurred with annual periodicity and growth lines were produced during each summer.

Muted indicators of methane production and oxidation have also been observed at discrete levels within the Cretaceous sediments on Seymour Island. They include the occurrence of thyasirid, lucinid and solemyid bivalves, which are taxa known to host chemosymbiotic bacteria and occur at modern and Cretaceous sites of methane seepage (Kauffman et al., 1996). Burrow-filling carbonates are also sometimes present within these levels and have distinctly negative carbon isotope compositions (−24 to −58‰, Little et al., 2015). However, the Maastrichtian–Paleocene López de Bertodano Formation on Seymour Island lacks the abundant authigenic carbonate which characterizes many modern marine methane seeps, and which can also be found in stratigraphically older early Maastrichtian sediments on nearby Snow Hill Island

(Little et al., 2015). This lack of authigenic carbonate (typically the burial product of sedimentary methane oxidation) suggests that the methane production and oxidation system in the Seymour Island region may have differed substantially from modern marine systems. One potential difference may have been the concentration of marine sulfate which plays a particularly important role in the marine methane cycle as discussed below.

The sedimentary production and release of methane is largely a function of the depth of penetration of various oxidants into marine sediments. In the modern ocean, sulfate plays a key role in the oxidation of organic carbon in ocean sediments via microbial sulfate reduction (MSR), which can account for up to ~80% of organic carbon oxidation (Jørgensen and Kasten, 2006). Only organic carbon that survives oxidation by MSR at sedimentary depths where sulfate concentrations have been reduced to zero is then available for methanogenesis. Once methane is produced it diffuses upwards until it encounters dissolved sulfate in porewaters where it is almost wholly consumed via sulfate fueled anaerobic oxidation of methane (AOM, Knittel and Boetius, 2009). Ocean sulfate concentrations will, therefore, exert a first order control on sedimentary methane production by affecting both the amount of organic carbon available for methanogenesis, and the depth in the sediment at which methanogenesis becomes the dominant fate for this carbon.

Estimates of marine sulfate concentrations from halite fluid inclusions, sulfur isotope rate of change calculations and geochemical models suggest that the Maastrichtian–early Paleocene time period (approximately 69 to 65 Ma) examined in this study was likely to have been characterized by ocean sulfate concentrations far lower than modern seawater (Table 1; modern seawater = 29 mM). Of particular note is the estimate from sulfate isotope rate of change calculations performed on a carbonate associated sulfate–sulfur isotope record derived from the same Seymour Island succession used in this study, which indicates that the maximum sulfate concentration for this time interval was ~2 mM (Witts et al., 2018). This is at the bottom end of the range of estimates produced by other methods, although there are no data from Maastrichtian halite fluid inclusions for a direct comparison. The temporally closest halite fluid records are of Aptian and Albian–Cenomanian age (125 to 93.9 Ma) with a range of sulfate concentrations between 5 and 16 mM (Lowenstein et al., 2003; Timofeeff et al., 2006), and the Eocene and Oligocene (56 to 23 Ma) with sulfate concentrations between 14 and 23 mM (Horita et al., 2002). This suggests that marine sulfate concentrations began to rise significantly after the K–Pg boundary. Modeling studies also give similar intermediate marine sulfate concentrations for the Maastrichtian with estimates from ~5 to ~15 mM (Wortmann and Paytan, 2012; Berner, 2004; Demicco et al., 2005). Taken together, this evidence strongly suggests that, while the exact concentration of sulfate in the Late Cretaceous is uncertain, concentrations were likely to have been less than half that of modern seawater (i.e. ~14 mM).

It is therefore reasonable to hypothesize that lower sulfate oceans of the Late Cretaceous would have been characterized by greater methane production, with methanogenesis occurring at

Table 1

A compilation of marine sulfate concentration estimates for the Maastrichtian and additional temporally closest data sets using a variety of methods.

Age (Ma)	SO ₄ (mmol/kg H ₂ O)	Method	References
37–35	12–23	Halite fluid inclusion	Horita et al. (2002)
69–65	~5	Modeling	Wortmann and Paytan (2012)
69–65	~11	Modeling	Berner (2004)
69–65	~15	Modeling	Demicco et al. (2005)
69–65	≤2	S-isotope rate of change	Witts et al. (2018)
100.5–89.8	2–7	S-isotope rate of change	Adams et al. (2010), Owens et al. (2013)
125–93.9	5–16	Halite fluid inclusion	Lowenstein et al. (2003), Timofeeff et al. (2006)

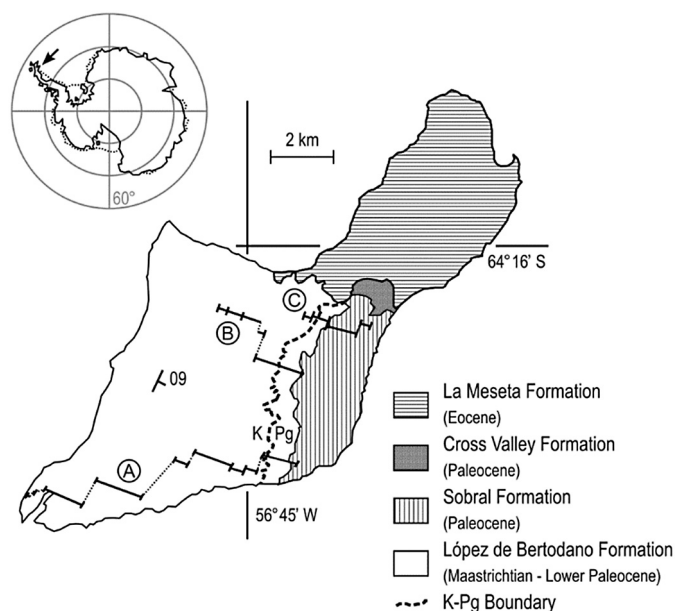


Fig. 1. Modern geographic index map and geologic map of Seymour Island. Major stratigraphic units coded by shading. Section lines; (A) AFI 2004 composite D5.251 (Bowman et al., 2014); (B) BAS 1999 composite DJ.959-957-953-952 (Crame et al., 2004); (C) D9 BAS 2010 composite D9.205-206-207-209-210-211 (Crame et al., 2014).

shallower depths in the sediment. The result is likely to have been an increased flux of methane across the sediment–water interface (Wortmann and Chernyavsky, 2007; Wortmann and Paytan, 2012), and increased methane-derived DIC with a characteristic negative $\delta^{13}\text{C}$ signature in bottom-waters. This DIC signal has the potential to be detected in shell carbonate and is used here to explore the evidence for an increased flux of methane and potential links to low marine sulfate concentrations.

2. Methods

2.1. Location

Fossils from the López de Bertodano Formation of Seymour Island (Fig. 1) were used for this study. The formation has well-defined stratigraphy and abundant macrofossil content in addition to some indications of the presence of methane near the sediment–water interface. A robust age model for the López de Bertodano Formation has been established using a combination of strontium isotope chemostratigraphy (McArthur et al., 1998; Crame et al., 2004), marine palynology (Elliot et al., 1994; Bowman et al., 2012) and magnetostratigraphy (Tobin et al., 2012). This age model constrains the bivalve-rich, upper strata of the formation to Maastrichtian to early Paleocene in age (~69 to 65 Ma; Bowman et al., 2013; Witts et al., 2016 and references therein).

The López de Bertodano Formation represents a shallow marine shelf setting, with water depths of 50 to 200 m (Macellari, 1988; Crame et al., 2004), located at a paleolatitude of 65°S (Lawver et al., 1992). Paleomagnetic dating suggests accumulation rates of 0.01 to 0.02 cm/yr (Tobin et al., 2012), which are within normal marine sedimentation rates, albeit at the upper end (e.g. Ibach, 1982). The sedimentology ranges from clayey silts to silty clays, with occasional glauconite beds signaling temporary reductions in the rate of deposition (Zinsmeister, 1998). Macrofauna, microfauna and trace fossils are abundant and diverse throughout the section, with many species found to persist up to the K–Pg boundary (e.g. Zinsmeister, 1998; Tobin et al., 2012; Witts et al., 2016). Specimens

were collected from several measured stratigraphic sections across southern Seymour Island (Fig. 1 and Supplementary Material).

2.2. Preservation

Fossil bivalves were examined using multiple techniques to confirm preservation of the original aragonite shell material and rule out diagenetic resetting of stable isotopes. Eleven specimens were examined on a cold cathode cathodoluminescence system (CITL 8200 Mk 3A mounted on a Nikon Optiphot petrological microscope) to identify areas of Mg-rich carbonate reprecipitation. The shell microstructure of five specimens was examined under scanning electron microscope as polished and etched polyester resin-mounted blocks or as fractured surfaces. Eight bulk powders collected by MicroMill from different shell layers were analyzed using X-ray diffraction (Bruker D8 diffractometer scanning from 20° to 60° with a 0.02° step size) and Topas software to indicate proportions of aragonite and calcite. Standard methodology was used for all analyses. Diagenetic alteration to calcite was found to be limited to the surface layers only (where found at all), and shells were polished or sectioned for sampling to minimize contamination. Full preservation test results are presented in the Supplementary Material.

2.3. Shell carbonate analysis

High resolution stable carbon and oxygen isotope microanalysis was performed on 18 well-preserved specimens. *Lahillia* were polished by Dremel to remove any surface alteration and sampled on the outer surface. *Cucullaea* were sectioned along the line of maximum growth and sampled from the cut face to avoid the intermittent periostracal layer identified by SEM (Fig. S2). Specimens were microsampled following standard procedures (Dettman and Lohmann, 1995) using a Merchantek MicroMill at a resolution of between 5 and 10 samples per visible growth increment. The $\delta^{18}\text{O}$ and $\delta^{13}\text{C}$ compositions of the resulting powders were determined using a Micromass Multicarb Sample Preparation System attached to a VG SIRA Mass Spectrometer. The results are reported with reference to the international standard V-PDB and the precision is better than $\pm 0.06\text{‰}$ for $\delta^{13}\text{C}$ and $\pm 0.08\text{‰}$ for $\delta^{18}\text{O}$. A total of 12 *Lahillia* and 6 *Cucullaea* were successfully sampled at high resolution. Bulk shell powders produced by grinding shell fragments from a further 34 *Lahillia* and 8 *Cucullaea* were also tested for stable isotope composition following the same method.

2.4. Sediment analysis

A total of 133 samples of bulk sediment from section D5.251 were analyzed for organic carbon isotope content, total organic carbon (TOC) and carbonate content. Samples were prepared by acidification following standard techniques to remove all carbonate and non-organic material (see Supplementary Material) and analyzed using an Isoprime mass spectrometer coupled to a Eurovector or Elementar Pyrocube elemental analyzer. $^{13}\text{C}/^{12}\text{C}$ ratios were calibrated using the international standards ANU-sucrose and IAEA-CH7 to the V-PDB scale with a precision of better than $\pm 0.25\text{‰}$ for repeat analysis of standard materials during the runs. Calculation of weight percent organic carbon was either derived from the mass spectrometer traces or analyzed on a LECO elemental analyzer, and corrected for weight loss during the acidification process. Weight percent carbonate was either calculated from weight loss during acidification or from analyzing total carbon on the LECO and then calculating total inorganic carbon (TIC) by deducting TOC. TIC was then converted to weight percent carbonate by assuming that it was all present as CaCO_3 .

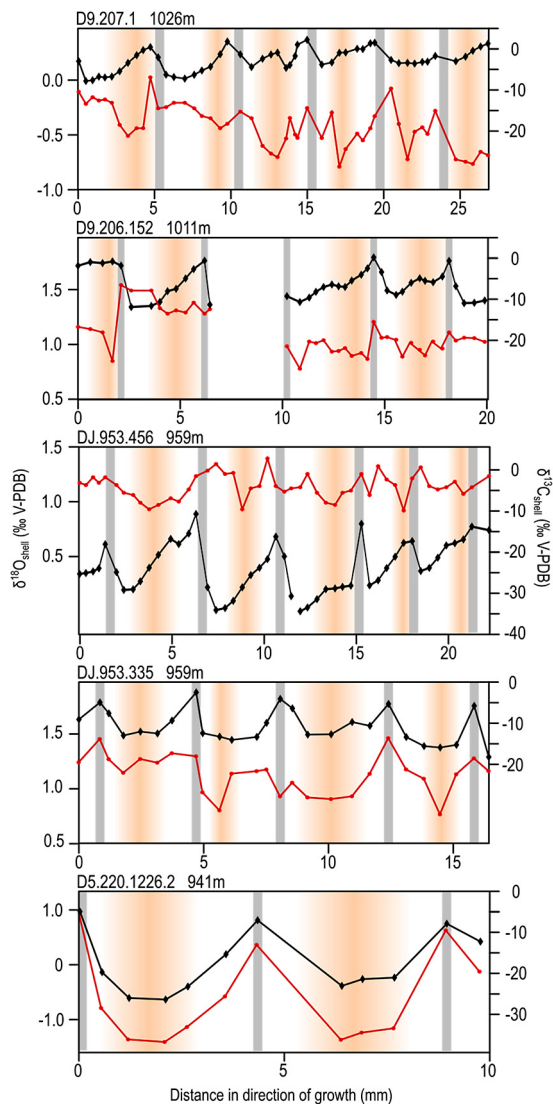


Fig. 2. Stable isotope shell profiles of selected *Lahillia* specimens showing large amplitude $\delta^{13}\text{C}$ variability and associated $\delta^{18}\text{O}$ data. Stable oxygen (red dots, left axis) and carbon (black diamonds, right axis) isotopes plotted using comparable vertical scales. Specimen number and stratigraphic height of each specimen are shown. Distance axis begins at an arbitrary point within the shell. Vertical gray bars locate positions of visible growth lines. Orange shading highlights the peak $\delta^{18}\text{O}$ values. Analytical reproducibility of $\pm 0.06\text{‰}$ for $\delta^{13}\text{C}$ and $\pm 0.08\text{‰}$ for $\delta^{18}\text{O}$ do not plot at this resolution. (For interpretation of the colors in the figure(s), the reader is referred to the web version of this article.)

3. Results

The preservation of original aragonitic shell microstructures was confirmed by a combination of scanning electron microscopy, cathodoluminescence imaging and X-ray diffraction analysis (refer to Supplementary Material for further details). The presence of the original microstructures suggests that little alteration has occurred, as they would likely have been obliterated during any wholesale isotopic resetting by dissolution and re-precipitation. Oxygen isotopic values in all specimens range from 2.84 to -4.44‰ , and were used to establish the seasonal timing of the carbon isotopic data. More negative carbonate- $\delta^{18}\text{O}$ is a relatively common feature of the mid to late portion of the growth increment in both species although the most negative value can occur at almost any point within a given growth increment. Smooth cusped trajectories truncated against visible major growth lines are sometimes distinguishable (Fig. 2). The $\delta^{18}\text{O}$ records often have considerable

scatter between consecutive points sampled within the shell but broad trends can be discerned. Point-to-point change is mostly larger than analytical uncertainty of up to $\pm 0.08\text{‰}$ (see Supplementary Material).

Microsampled carbonate- $\delta^{13}\text{C}$ results range from $+6.3$ to -34.2‰ (Fig. 2 and dataset S2) across all specimens sampled. The average and range of carbonate- $\delta^{13}\text{C}$ within each shell also varies markedly (average from $+4.2$ to -23.8‰ , range from 0.4 to 23.5‰). The shells with the most negative means and the largest ranges of carbonate-carbon isotope composition appear to be from particular stratigraphic intervals (notably 930 to 970 m and 1000 to 1040 m). Regular patterns of change within each growth increment are also observed in the shell $\delta^{13}\text{C}$ records. In specimens with the largest carbon isotope ranges, more negative carbonate- $\delta^{13}\text{C}$ data points are generally found in earlier parts of the growth period and more positive $\delta^{13}\text{C}$ immediately before or within each dark growth ring. No clear pattern is apparent in the specimens that record a smaller range of $\delta^{13}\text{C}$, with some shells presenting the most positive $\delta^{13}\text{C}$ at each growth line, and some the most negative.

Percentages of total organic carbon (TOC) range between 0.14 and 0.65% throughout the succession (Fig. 3) with an average value of 0.38 wt%. Organic-carbon $\delta^{13}\text{C}$ ranges from -21.7 to -26.1‰ with an average of -24.8‰ and no clear stratigraphic trend. Weight percent carbonate varies between 6.3 and 22.0%, with a particularly carbonate-rich horizon at the K-Pg boundary, which is likely to be related to a glauconite-rich layer at the same position (Zinsmeister, 1998). Neither TOC, organic- $\delta^{13}\text{C}$, or weight percent carbonate display any correlation with the stratigraphic intervals containing the shells with the most negative average carbonate- $\delta^{13}\text{C}$.

4. Discussion

4.1. Shell carbonate $\delta^{18}\text{O}$ signal

The origin of the scattered nature of the $\delta^{18}\text{O}$ shell data is unclear but may be a result of sample analysis error or depth attenuation of the surface-water temperature signal. Despite the scatter, there is an overall tendency for the most positive $\delta^{18}\text{O}$ compositions to occur at the growth lines, with more negative shell $\delta^{18}\text{O}$ recorded during the growth increments. This is consistent with a weak annual seasonal cycle with shell production throughout the warming spring and summer, but growth ceasing for the cold winter period. Most bivalves do not grow continuously year-round; it is typical for many species of mid-to-high latitude modern bivalves to pause growth for spawning, or when water temperatures are outside of a tolerated threshold range, producing annual growth lines (e.g. Schöne et al., 2005b). Eocene *Cucullaea* from Seymour Island also produced an annual growth line but in the warmer months rather than the cooler months (Buick and Ivany, 2004). This difference may have been a response to a warmer Eocene climate compared to the Late Cretaceous, causing bivalves to adjust shell production within a favorable temperature range (e.g. Jones and Quitmyer, 1996).

Averaged shell $\delta^{18}\text{O}$ data were converted to temperature data using standard aragonite conversions (Grossman and Ku, 1986; Schöne et al., 2005a, 2005b) using two values for seawater $\delta^{18}\text{O}$ (-1 and -1.5‰) estimated from model simulations and clumped isotope work (Petersen et al., 2016; Hall, 2017). This range of seawater values and conversion equations gave upper and lower temperature estimates between 19.0 and 5.1 °C across the set of specimens, of which approximately 2 °C was due to the water- $\delta^{18}\text{O}$ uncertainty in the conversion (further details can be found in the Supplementary Material). The presence of growth-line related signals in the $\delta^{18}\text{O}$ record also confirms the observed excellent

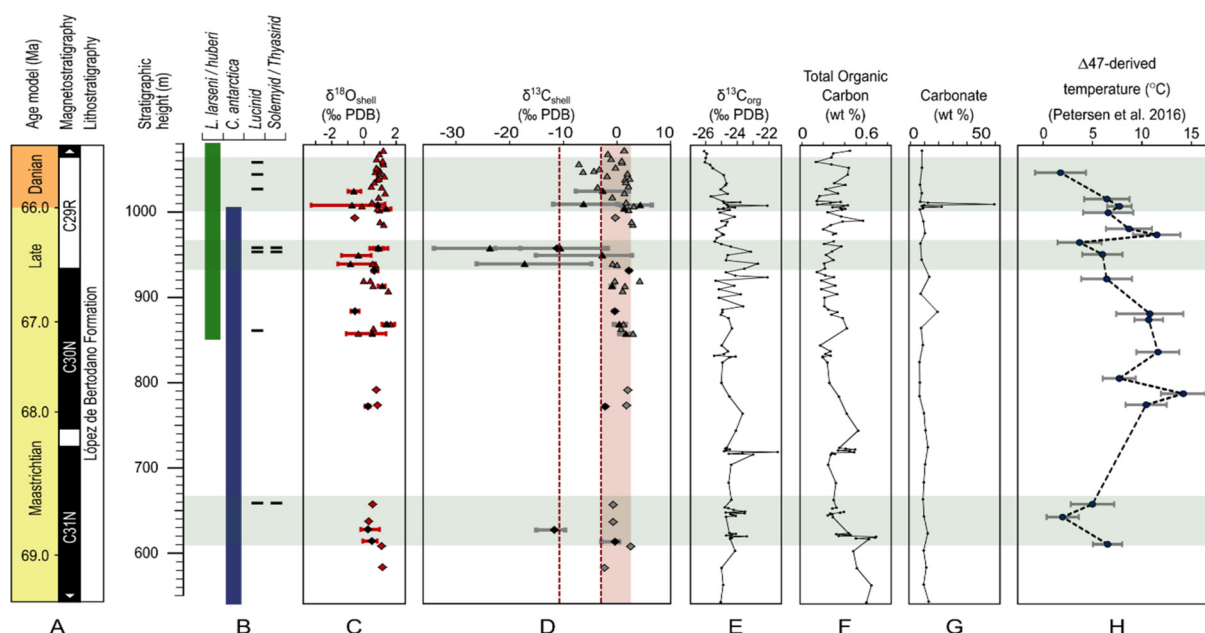


Fig. 3. Stable isotope data from Seymour Island. Horizontal green shading highlights intervals with indicators of methane influence. (A) Stratigraphic data; age model (Bowman et al., 2013), magnetostratigraphy (Tobin et al., 2012) and lithostratigraphy (Crame et al., 2004). Samples from each section have been correlated using a standardized stratigraphy with several tie-points including the K–Pg boundary at 1007.5 m (Witts et al., 2016). (B) Stratigraphic ranges for selected bivalve species including recorded horizons of chemosymbiotic-associated lucinids, thyasirids and solemyids (Little et al., 2015). (C–D) Bulk $\delta^{18}\text{O}$ and $\delta^{13}\text{C}$ values from *Lahillia* (triangles) and *Cucullaea* (diamonds), horizontal bars with black markers indicate the range and mean values from specimens sampled at high resolution and are not error bars; the shaded field represents the values within the range of expected shell $\delta^{13}\text{C}$ depletion due to metabolic carbon incorporation; dashed vertical lines represent shell $\delta^{13}\text{C}$ values calculated for normal (10%) and extreme (37%) fractional incorporation. (E–G) Bulk sediment results from composite section D5.251; organic carbon $\delta^{13}\text{C}$; weight percent total organic; weight percent carbonate. (H) $\Delta 47$ -derived temperature record from Seymour Island (Petersen et al., 2016) correlated with stratigraphy using the K–Pg boundary position.

preservation of these specimens and suggests that little isotopic resetting has occurred (Ivany, 2012).

4.2. Origins of the shell carbonate $\delta^{13}\text{C}$ signal

A large proportion of the carbonate- $\delta^{13}\text{C}$ data at the positive end of our data set (+6.3 to -34.2‰) are typical of modern marine heterotrophic bivalves (Toland et al., 2000; Carré et al., 2005; Schöne et al., 2005a) whilst the more negative data are difficult to explain under normal marine conditions and could be indicative of methane input to DIC.

Most shell carbonate-carbon is derived from bottom water DIC but some metabolic carbon can be incorporated from the organism's particulate organic carbon (POC) food source which typically has a negative $\delta^{13}\text{C}$ signature and could feasibly contribute to the negative $\delta^{13}\text{C}$ recorded by the shells. We used a simple isotopic mass balance to identify an expected range of $\delta^{13}\text{C}_{\text{shell}}$ compositions (+2.5 to -2.8‰) for this latitude and geological time period without any additional source of methane-derived DIC. This mass balance incorporated accepted values for metabolic carbon contribution to bivalve shells (F; 0 to 10%, McConnaughey et al., 1997; Poulain et al., 2010), isotope compositions of the POC food source ($\delta^{13}\text{C}_{\text{POC}}$; -28 to -20‰ , Mook and Tan, 1991), and Cretaceous ambient DIC ($\delta^{13}\text{C}_{\text{DIC}}$; 0 to $+2.5\text{‰}$, Voigt et al., 2012). Further details can be found in the Supplementary Material. Repeating the calculation using the most extreme incorporation of metabolic carbon reported in modern bivalves (37%, Gillikin et al., 2007) extends the lower limit of this $\delta^{13}\text{C}$ range to -10.4‰ .

$$\delta^{13}\text{C}_{\text{shell}} = F\delta^{13}\text{C}_{\text{DIC}} + (1 - F)\delta^{13}\text{C}_{\text{POC}}$$

Nine of the eighteen bivalves sampled produced at least one carbonate- $\delta^{13}\text{C}$ value more negative than the normal $+2.5$ to -2.8‰ range. Within these nine shells, the mean average shell

$\delta^{13}\text{C}$ ranges from -23.8 to -0.5‰ . Six out of these nine also contain at least two $\delta^{13}\text{C}$ values more negative than our calculated limit on shell carbonate- $\delta^{13}\text{C}$ produced by exceptional incorporation of metabolic carbon (-10.4‰). Large seasonal cycles in carbon isotopes are a further remarkable feature of this subset of nine shells with the range of $\delta^{13}\text{C}$ recorded within a single shell varying between 3.3 and 23.5‰. The most negative annual carbonate- $\delta^{13}\text{C}$ compositions are typically found at the beginning of each growth increment with a gradual return to less negative values throughout the growing period; and more positive $\delta^{13}\text{C}$ at each growth line (Fig. 2).

Given that our preservation tests and $\delta^{18}\text{O}$ observations show that post-depositional alteration is not a credible explanation for the extreme seasonal $\delta^{13}\text{C}$ variability, we need to consider alternate hypotheses for their origin. We suggest that the most likely source of the ^{13}C -depleted carbon in the affected bivalve shells is methane-derived carbon, since methane can provide a much more negative range of $\delta^{13}\text{C}$ signatures than photosynthetic-derived POC (Whiticar, 1999).

The remaining nine shells sampled at high resolution have much more typical $\delta^{13}\text{C}$ averages of between -2.3 and $+4.2\text{‰}$, and while seasonal variability is still present, the range of values represented within the whole shell is much lower; between 0.4 and 5.8‰. Slight negative correlation can be observed in some cases between $\delta^{18}\text{O}$ and $\delta^{13}\text{C}$ (i.e. low $\delta^{13}\text{C}$ and high $\delta^{18}\text{O}$ at each growth line). This is typical of a shallow marine productivity signal, where summer productivity causes water $\delta^{13}\text{C}$ to become more positive and the associated warm water temperatures produce a more negative $\delta^{18}\text{O}$ signal (e.g. Toland et al., 2000; Carré et al., 2005; Schöne et al., 2005a). This lends support to the interpretation of a spring-summer duration for a single growth increment. A few shells record some anomalously positive $\delta^{13}\text{C}$ values. It is possible that these may reflect periods of very high biological productivity (Alcalá-Herrera et al., 1992; Gillikin et al., 2007) or local diagenetic effects due to cracks or microborings. Al-

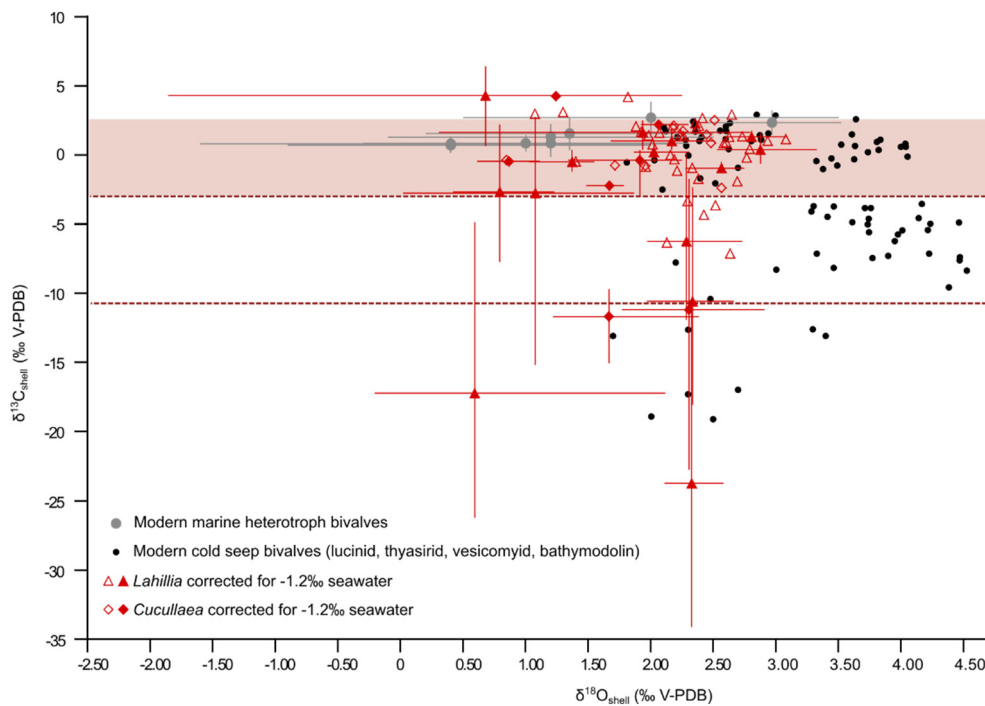


Fig. 4. Bulk and average shell carbonate carbon–oxygen cross-plot. Stable isotope data (red) from the heterotrophic bivalves *Lahillia* (triangles) and *Cucullaea* (diamonds). Horizontal and vertical range crosses with filled markers represent the mean and range of microsampled data points produced within one shell. Hollow markers represent bulk data from a single shell. $\delta^{18}\text{O}$ data from Seymour Island specimens have been shifted by $+1.2\text{‰}$ to account for the difference between modern seawater (0‰) and Cretaceous $\delta^{18}\text{O}_{\text{seawater}}$ (taken as -1.2‰ , Zachos et al., 2001). Red dashed line and shaded field represent expected Cretaceous shell $\delta^{13}\text{C}$ values calculated for normal (10%) and extreme (37%) fractional incorporation as in Fig. 3. This data is compared to modern bivalves from cold seeps (black circles, Lartaud et al., 2010) and modern marine heterotrophs (gray circles with range bars, Krantz et al., 1987; Toland et al., 2000; Schöne et al., 2005a). This shows that some of Seymour Island's bivalves display a similar isotopic pattern to normal marine bivalves, however the $\delta^{18}\text{O}$ indicates temperatures far warmer than most modern cold seep environments.

ternatively, the positive $\delta^{13}\text{C}$ signals may be caused by the addition of small amounts of residual ^{13}C -enriched CO_2 from sedimentary methane production expelled from porewaters by compaction.

Specimens that were analyzed as bulk shell powders, rather than microsampled across growth lines, also show some evidence for intervals of negative $\delta^{13}\text{C}$ (Fig. 3) with 6 of the 42 specimens sampled falling outside of our calculated normal marine shell carbonate $\delta^{13}\text{C}$ range. This shows that even when not temporally well-constrained by shell growth lines, the carbonate–carbon records are indicative of a strong benthic methane influence.

The carbonate– $\delta^{13}\text{C}$ data represent a continuum of behavior, from those which can be explained entirely without invoking methane-derived carbon, to those where methane-derived carbon makes a substantial contribution to the total shell carbonate. They are therefore suggestive of a variable or intermittent methane flux to the benthic environment, both on seasonal but also much longer timescales. The distinct stratigraphic intervals characterized by bivalves with ^{13}C -depleted shell signals occur close to, or overlap with occurrences of putatively chemosymbiotic bivalves (Fig. 3) (Little et al., 2015). This provides further support for the idea that the $\delta^{13}\text{C}$ signals in shells are indicative of an enhanced abundance of shallow sedimentary methane. However, observations of bulk sediment organic $\delta^{13}\text{C}$ data from the López de Bertodano Formation are within the modern Antarctic isotopic range of POC (as used in the mass balance calculation) and reveal no corresponding negative carbon isotope excursions concurrent with the episodes of more negative carbonate– $\delta^{13}\text{C}$ behavior in shells. This suggests that the bivalves recorded a signal localized in bottom-water DIC that did not propagate into the upper water column.

Shell $\delta^{13}\text{C}$ values of the magnitude we observed have not been recorded in any modern heterotrophic bivalves (Fig. 4). Even chemosymbiotic bivalves from modern and ancient methane seep sites show little ^{13}C depletion in their shell material (Kauffman et

al., 1996; Hein et al., 2006; Lartaud et al., 2010). The most negative $\delta^{13}\text{C}$ signatures in seep bivalves are from their soft tissues, suggesting that in modern seep environments the methane signal is typically incorporated from metabolic carbon rather than from methane-derived DIC (Paull et al., 1989; Fisher, 1995). Cross plots $\delta^{18}\text{O}$ and $\delta^{13}\text{C}$ shell-averages show no apparent temperature connection to the presence or absence of a methane-influenced signal and are indicative of warmer water temperatures than those found at modern cold seeps.

4.3. Extreme seasonality in bottom water DIC– $\delta^{13}\text{C}$

One of the most remarkable features of the shell-carbonate data is the magnitude of the probable seasonal fluctuations in $\delta^{13}\text{C}$, which reflect a similar variability in the bottom water DIC. Seasonal $\delta^{13}\text{C}$ variability of DIC may be introduced by variation of the $\delta^{13}\text{C}$ of the methane itself, or by seasonal modulation of the rate of methane production or methane release. Winter ^{13}C depletion of up to 10‰ has been observed in biogenic methane from marine sediments (Martens et al., 1986), but this is insufficient and with the opposite sense to the variations reported here, which can be as great as 23.5‰ , even within the truncated period of spring–summer shell growth.

Since variability of methane $\delta^{13}\text{C}$ is unlikely to fully explain the observed signals, we consider mechanisms by which methane flux may be pulsed annually. Annual temperature changes are known to trigger seasonal methane release from methane hydrates in modern high latitude marine settings (Berndt et al., 2014). However, the sedimentology and faunal assemblage of the López de Bertodano Formation suggest a continental shelf setting with water depths of between 50 and 200 m (Macellari, 1988; Crame et al., 2004). Under these conditions, sea-bed hydrates would only have been stable at mean-annual temperatures lower

than -2°C (Kvenvolden, 1993). This is far colder than the existing temperature estimates from this region (Kemp et al., 2014) or the temperatures derived from the carbonate- $\delta^{18}\text{O}$ data reported here (19.0 to 5.1°C).

Recent work covering the same latest Cretaceous to Paleogene interval of the López de Bertodano Formation (Petersen et al., 2016) has provided evidence for temperatures significantly cooler than produced by our study. Whilst correlation between the two datasets is likely to be imprecise due to differences in collection methods and the calculation of relative position in stratigraphy, there does seem to be some coincidence between lower clumped isotope temperature estimates and our intervals of more negative shell carbonate- $\delta^{13}\text{C}$ (Fig. 3). We carried out one-dimensional sedimentary geotherm modeling to determine whether the lower temperature estimates indicated by the clumped isotope proxy used would have been sufficient to allow sedimentary hydrate formation. The results of this investigation (see Supplementary Material for details) show that even at the lowest temperatures recorded in the Petersen study by *Lahillia* and *Cucullaea* no hydrates could have been formed at depths that could have been realistically affected by seasonal variations in temperature and pressure. From this we can conclude that hydrates were not likely to have been involved in the production or seasonality of the methane signal.

Additionally, the stratigraphic occurrences of the putatively chemosymbiotic fauna (Fig. 3) occur across multiple section lines spaced 2–6 km apart. Samples showing evidence for methane-influence are sourced from across all sections. The spatial distribution of these signals across several kilometers of the shelf environment also favors a mechanism generated by a wider change in sediment biogeochemistry rather than focused methane seepage which tends to be more localized. We conclude that the bivalve shells were most likely recording a direct signal of enhanced springtime methane input to bottom-water DIC directly from the shelf sediment. The ^{13}C -depletion in bottom-water DIC must have been due to some combination of enhanced methane production or release and eventual oxidation to DIC.

Modern areas of prolific seasonal methane production and release tend to occur in shallow waters such as swamps and marginal marine sites with extremely high organic carbon sedimentation, many of which also have sulfate concentrations lower than fully marine environments (Crill and Martens, 1983; Van der Nat and Middelburg, 2000; Zhang et al., 2008). Today, seasonal methane production in the marine environment is limited to shallow sites with marked annual temperature variability, annual stratification, or high sedimentation rates coupled to high organic input. The temperature sensitivity of methanogenesis is well known, and provides a primary reason why shallow sites may exhibit seasonal variability in methane production (Zeikus and Winfrey, 1976; Crill and Martens, 1983).

We are unaware of any modern marine shelf settings with similar depths to those in our study with evidence for an annually modulated bottom-water methane flux. Our discovery of evidence for seasonal methane release in a relatively deep high-biodiversity fully-marine environment without indication of high sedimentary TOC supports the interpretation that Cretaceous marine sediments may have had a more sensitive methane cycle. Given the relatively deep nature of the Seymour Island succession, and the limited seasonal temperature range suggested by the shell carbonate- $\delta^{18}\text{O}$, it is likely that temperature only plays a minor role in the seasonal control of the methane cycle in this case.

In high latitude settings in a greenhouse world with a vegetated and temperate Antarctic continent, coastal waters are likely to have experienced a build-up of surface water nutrients during the dark winter months and a spring pulse of runoff into coastal waters. The nearest modern-world analogue to such a system might be north Norwegian fjords, which have a vegetated hinterland and

a high latitude light regime, but relatively warm water temperatures (Wassmann et al., 1996). In these systems, there are two phytoplankton blooms; the first relating to the increasing light intensity in the spring, and the second to the influx of meltwater. Both events result in marked increases in organic matter delivery to the sediment (Wassmann et al., 1996).

Seasonal addition of organic particulate carbon to surface sediments can directly stimulate methanogenesis in modern lake systems because sulfate and other electron acceptors are not very abundant. Organic carbon addition to the sediment surface can also rapidly stimulate methane production deeper in the sediment by the diffusion of dissolved labile organic matter (Borrel et al., 2011). In the Seymour Island shelf sediments, sulfate is likely to have been too high compared to terrestrial freshwater lake systems to allow the former, but a lower marine sulfate concentration would have shallowed the zone of methane production compared to modern shelf sediments (Fig. 5). We speculate that the shallower depth of methanogenesis could have brought it within reach of this downwards diffusion of dissolved organics and may have allowed methane production to respond to bloom-derived pulses of organic-carbon to the sediments. The combined likelihoods of distinctly pulsed organic matter delivery linked to the high latitude setting, an ocean with a reduced sulfate concentration ocean, and shallowing of the methanogenic zone make seasonal control by organic carbon flux a plausible mechanism.

An alternative to a seasonal control on the production of marine methane could have been a seasonal modulation of its release and oxidation by some physical disturbance, perhaps by changing storm frequency. Whilst it is not possible to conclusively distinguish between these mechanisms with the available data, a low sulfate ocean and shallowing of the methanogenic zone would make all proposed mechanisms more conceivable by bringing methanogenesis and its products closer to the influence of processes operating at the sediment–water interface.

4.4. Contribution of methane to bottom water DIC

Extending the mass balance approach introduced earlier allows us to produce an estimate of the amount of methane-derived carbon required to produce shell carbonate signals as depleted as we observe here. A similar mass balance equation (below) was used to determine the amount of methane derived DIC required to produce the bottom-water DIC signal we infer from our $\delta^{13}\text{C}_{\text{shell}}$ data. Using typical $\delta^{13}\text{C}$ for biogenic methane of -50 to -110‰ (Whiticar, 1999), these calculations suggest that between 30 and 85% methane derived DIC is required to account for the most extreme negative shell values. Further details and results tables for all calculations are available in the Supplementary Material (Tables S1 to S3).

$$\begin{aligned} \delta^{13}\text{C}_{\text{bottom water DIC}} \\ = F\delta^{13}\text{C}_{\text{methane-derived DIC}} + (1 - F)\delta^{13}\text{C}_{\text{oceanic DIC}} \end{aligned}$$

The strength of the isotopic signals is consistent with our original hypothesis that the low-sulfate conditions of the Cretaceous–Paleocene allowed for a greatly increased flux of methane-derived DIC to bottom-waters. A conceptual model of the normal modern and hypothetical low-sulfate conditions is proposed in Fig. 5. The inferred isotopically-depleted carbon in bottom-water DIC recorded by the bivalve shells is likely to have resulted from some combination of enhanced methane production or release and its oxidation to bottom-water DIC, but it would be challenging to decouple these effects.

In the modern ocean the vast majority of methane produced in sediment is oxidized anaerobically by sulfate (sulfate driven AOM,

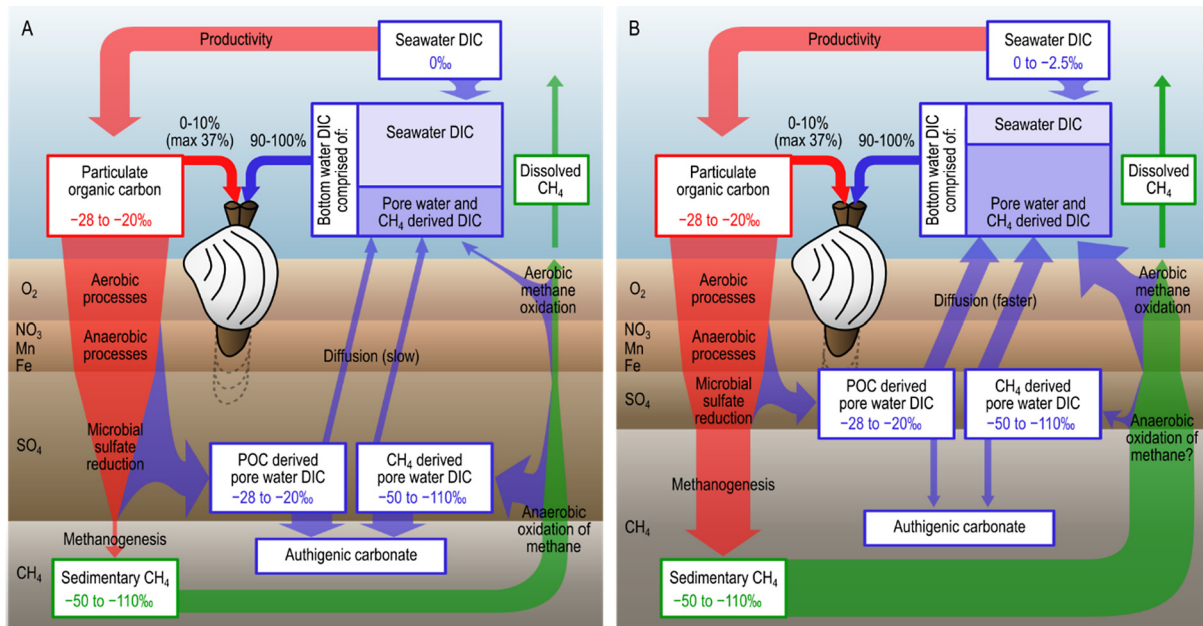


Fig. 5. Conceptual model of sedimentary carbon cycle under high and low sulfate conditions. Conceptual diagram of fluxes of POC (red), DIC (blue) and methane (green) under (A) modern high sulfate conditions, (B) Cretaceous lower sulfate conditions. Thickness of arrows represents relative strength of flux to each reservoir (not to scale). Depth scales are arbitrary; bottom-water reservoir refers to the benthic boundary layer sampled by bivalves and is likely to be only 5–10 cm in depth. The depth to the sulfate reduction zone is variable in modern marine sediments depending on factors such as diffusion and bioturbation. The proportion of pore water DIC that diffuses into bottom water versus burial as authigenic carbonate is unknown, but likely to relate to depth of DIC production, and pore fluid flux from the sediment to bottom water, thus is likely to be faster in low sulfate systems. No significant accumulations of authigenic carbonate have been found at horizons where we see evidence for increased methane flux to bottom-water DIC.

Reeburgh, 2007). Although we calculate a large contribution of oxidized methane to bottom-water DIC, it would be challenging to determine the proportion of this methane-derived DIC produced by AOM versus aerobic oxidation of methane. It has also recently been shown that AOM can be facilitated by other electron acceptors such as iron (e.g. Ettwig et al., 2016) further complicating the issue. Various consequences of a lower sulfate ocean would come into play in determining how these microbial processes would interact. The shallowing of methane production would bring reactive sedimentary organic matter into competition with methane as a substrate, but this could also bring methane into contact with a greater supply of reactive iron oxides, perhaps making iron-driven AOM more likely under low sulfate concentrations. The exact controls on the occurrence and competition between various forms of AOM are the subject of considerable ongoing debate, leaving the exact response mechanisms in a marine setting with lower concentrations of sulfate unclear. Regardless, the lack of significant authigenic carbonate throughout the López de Bertodano Formation perhaps supports a reduced or minor role for either variety of AOM in total methane oxidation since AOM promotes authigenic carbonate precipitation whilst aerobic oxidation does not (Reeburgh, 2007). If most of the oxidation is being driven by oxygen, then the large proportion of methane derived DIC we calculate has significant implications for the bottom water oxygen budget, and may indicate that low sulfate conditions indirectly provided a substantial driver for bottom water de-oxygenation. Clearly, the continued presence of a diverse benthic fauna throughout the López de Bertodano Formation limits the significance of this process in our study section over long time scales, but is consistent with evidence of transient sedimentary anoxia from geochemical proxies (Witts et al., 2016; Schoepfer et al., 2017).

The episodic nature of seasonal methane release throughout the stratigraphic section is difficult to explain, as an increased methane flux due to a low sulfate biogeochemical regime might be expected to operate throughout this interval of geological time. It is possible that the onset of increased methane flux to DIC may have been influenced by a period of local climate warming observed through

the very latest Maastrichtian part of this section (Tobin et al., 2012; Bowman et al., 2013; Kemp et al., 2014; Petersen et al., 2016). We observe no correlation between increased $\delta^{18}\text{O}$ -temperature and the presence of ^{13}C depletion in shells from cross-plots (Fig. 4), and the temperature sensitivity of methanogenesis is not consistent with the approximate coincidence of the lower reported clumped isotope temperatures (Fig. 3), so it is unlikely that temperature was the primary driver of the methane flux. Periods of elevated sedimentation rate could also increase pore fluid flux; recent studies of modern passive margins (Prouty et al., 2016) suggest that high sedimentation rates, such as those present in the Cretaceous–Paleocene James Ross Basin (up to 0.01–0.02 cm/yr), may enhance pore space compaction and allow more methane or methane derived DIC to be expelled from sediments. It is also possible that the system in this location was balanced such that small changes in the regional sulfate concentration of the ocean may have driven the change in regime seen here.

Given the prevalence of low sulfate conditions through the Phanerozoic (Holt et al., 2014), the question arises as to why similar extreme shell carbon values have not been documented in studies of other geological ages. It is likely that unusual isotopic signals from single analyses of bulk shell material have been discounted as the result of poor preservation, preparation or a productivity signal (Lartaud et al., 2010; Tobin and Ward, 2015), especially if, as is seen here, the signals are sporadic in nature and only present in a subset of shells analyzed. Indeed, similarly negative $\delta^{13}\text{C}$ data have been reported from the bulk shell carbonate of a number of ammonites, gastropods, and calcitic and aragonitic bivalves from Seymour Island and dismissed as sample preparation error (Tobin and Ward, 2015). Our method of micro-analysis lends confidence to the primary nature of the signals and allows the repetitive seasonal patterns within shells to be identified. This approach is rarely used for fossil shell material, but may be required in order to detect the extreme seasonal signals that we have used in our calculations to provide diagnostic indicators of methanogenic input to bottom water DIC.

5. Conclusions

Isotopic records from latest Cretaceous and early Paleocene bivalves from Antarctica represent the first time that negative carbon isotope signals of this nature have been documented in the fossil record and resolved on a sub-annual scale, revealing both their seasonal and stratigraphically-pulsed characteristics. The shell carbonate–carbon signals are likely to be reflective of localized DIC composition, with extreme springtime carbon isotope depletion suggesting a very large contribution to bottom-water DIC by methane oxidation products. Bulk sediment organic-carbon isotopes indicate that the influence of this process did not extend to the upper water column.

The presence of pronounced annual cyclicity suggests intervals of strong environmental control on the flux of methane derived carbon to the bottom-water DIC pool. A methane hydrate mechanism appears unlikely at the temperatures and water depths indicated for this site, so the signal must be due to some combination of enhanced methane production or release and its subsequent oxidation, facilitated by the low sulfate concentrations of the Cretaceous–Paleocene ocean and the shallowing of the methanogenic zone. The limited variability in the shell oxygen-isotope record makes a temperature control unlikely but the high-latitude light regime and vegetated hinterland make a control by spring bloom fueled pulses of organic carbon more plausible.

The lack of substantial authigenic carbonate supports an aerobic oxidation pathway for the methane which has the potential to impact substantially on bottom water oxygen budgets and may be a driver for transient anoxia. If a low sulfate ocean was indeed a requirement for these unusual isotopic records then similar seasonal signals in shell carbonate are likely to be recorded in other low sulfate intervals of the Phanerozoic, and signify a fundamental difference in marine sedimentary carbon cycling in the past.

Acknowledgements

JLOH thanks the Natural Environment Research Council (NERC) UK for supporting her with a PhD studentship (NE/L501542/1). This work was also funded by NERC grants NE/C506399/1, NE/I005803/1, NE/I00582X/1 and NE/N018559/1. We thank Simon Crowhurst, James Rolfe, Tony Dickson, Oscar Branson, Giulio Lampronti (University of Cambridge), John Craven (University of Edinburgh) and Hilary Blagborough (British Antarctic Survey) for their assistance during data collection, and Vanessa Bowman (British Antarctic Survey) and Jon Ineson (Geological Survey of Denmark and Greenland) for use of their stratigraphic data. We are grateful for conversations with Ben Mills, Christian März, Johan Faust, and the Palaeo@Leeds research group. Special thanks also go to Linda Ivany, Aubrey Zerkle and one other anonymous reviewer for their thoughtful comments, which greatly improved the final version of the manuscript.

Appendix A. Supplementary material

Supplementary material related to this article can be found in the Supplementary Material file and Datasets S1 to S4 at <https://doi.org/10.1016/j.epsl.2018.06.014>.

References

- Adams, D.D., Hurtgen, M.T., Sageman, B.B., 2010. Volcanic triggering of a biogeochemical cascade during Oceanic Anoxic Event 2. *Nat. Geosci.* 3 (3), 1–4.
- Alcalá-Herrera, J.A., Grossman, E.L., Gartner, S., 1992. Nannofossil diversity and equitability and fine-fraction $\delta^{13}\text{C}$ across the Cretaceous/Tertiary boundary at Walvis Ridge Leg 74, South Atlantic. *Mar. Micropaleontol.* 20 (1), 77–88.
- Berndt, C., Feseker, T., Treude, T., Krastel, S., Liebetrau, V., Niemann, H., Bertics, V.J., Dumke, I., et al., 2014. Temporal constraints on hydrate-controlled methane seepage off Svalbard. *Science (NY)* 343 (6168), 284–287.
- Berner, R.A., 2004. A model for calcium, magnesium and sulfate in seawater over Phanerozoic time. *Am. J. Sci.* 304 (5), 438–453.
- Borrel, G., Jézéquel, D., Biderre-Petit, C., Morel-Desrosiers, N., Morel, J.P., Peyret, P., Fonty, G., Lehours, A.C., 2011. Production and consumption of methane in freshwater lake ecosystems. *Res. Microbiol.* 162 (9), 833–847.
- Bowman, V.C., Francis, J.E., Riding, J.B., Hunter, S.J., Haywood, A.M., 2012. A latest Cretaceous to earliest Paleogene dinoflagellate cyst zonation from Antarctica, and implications for phytoprovincialism in the high southern latitudes. *Rev. Palaeobot. Palynol.* 171, 40–56.
- Bowman, V.C., Francis, J.E., Riding, J.B., 2013. Late Cretaceous winter sea ice in Antarctica? *Geology* 41 (12), 1227–1230.
- Bowman, V.C., Francis, J.E., Askin, R.A., Riding, J.B., Swindles, G.T., 2014. Latest Cretaceous–earliest Paleogene vegetation and climate change at the high southern latitudes: palynological evidence from Seymour Island, Antarctic Peninsula. *Palaeogeogr. Palaeoclimatol. Palaeoecol.* 408, 26–47.
- Buick, D.P., Ivany, L.C., 2004. 100 years in the dark: extreme longevity of Eocene bivalves from Antarctica. *Geology* 32 (10), 921.
- Carré, M., Benteleb, I., Blamart, D., Ogle, N., Cardenas, F., Zevallos, S., Kalin, R.M., Ortlieb, L., et al., 2005. Stable isotopes and sclerochronology of the bivalve *Mesodesma donacium*: potential application to Peruvian paleoceanographic reconstructions. *Palaeogeogr. Palaeoclimatol. Palaeoecol.* 228 (1–2), 4–25.
- Crame, J.A., Francis, J.E., Cantrill, D.J., Pirrie, D., 2004. Maastrichtian stratigraphy of Antarctica. *Cretac. Res.* 25 (3), 411–423.
- Crame, J.A., Beu, A.G., Ineson, J.R., Francis, J.E., Whittle, R.J., Bowman, V.C., 2014. The early origin of the Antarctic marine fauna and its evolutionary implications. *PLoS ONE* 9 (12), e114743.
- Crill, P.M., Martens, C.S., 1983. Spatial and temporal fluctuations anoxic coastal marine sediments of methane production in anoxic coastal marine sediments. *Limnol. Oceanogr.* 28 (6), 1117–1130.
- Demico, R.V., Lowenstein, T.K., Hardie, L.A., Spencer, R.J., 2005. Model of seawater composition for the Phanerozoic. *Geology* 33 (11), 877–880.
- Dettman, D.L., Lohmann, K.C., 1995. Microsampling carbonates for stable isotope and minor element analysis; physical separation of samples on a 20 micrometer scale. *J. Sediment. Res.* 65 (3a), 566–569.
- Elliot, D.H., Askin, R.A., Kyte, F.T., Zinsmeister, W.J., 1994. Iridium and dinocysts at the Cretaceous–Tertiary boundary on Seymour Island, Antarctica: implications for the K–T event. *Geology* 22 (8), 675.
- Ettwig, K.F., Zhu, B., Speth, D., Keltjens, J.T., Jetten, M.S.M., Kartal, B., 2016. Archaea catalyze iron-dependent anaerobic oxidation of methane. *Proc. Natl. Acad. Sci. USA* 113 (45), 12792–12796.
- Fisher, C., 1995. Toward an appreciation of hydrothermal-vent animals: their environment, physiological ecology, and tissue stable isotope values. In: Humphris, S.E., Zierenberg, R.A., Mullineaux, L.S., Thomson, R.E. (Eds.), *Seafloor Hydrothermal Systems: Physical, Chemical, Biological, and Geological Interactions*. In: *Geophys. Monogr.*, pp. 297–316.
- Gillikin, D.P., Lorrain, A., Meng, L., Dehairs, F., 2007. A large metabolic carbon contribution to the $\delta^{13}\text{C}$ record in marine aragonitic bivalve shells. *Geochim. Cosmochim. Acta* 71 (12), 2936–2946.
- Grossman, E.L., Ku, T.-L., 1986. Oxygen and carbon isotope fractionation in biogenic aragonite: temperature effects. *Chem. Geol.* 59, 59–74.
- Hall, J.L.O., 2017. Marine Bivalve Records of Antarctic Seasonality and Biological Responses to Environmental Change over the Cretaceous–Paleogene Mass Extinction Interval. PhD Thesis. University of Leeds.
- Hein, J.R., Normark, W.R., McIntyre, B.R., Lorenson, T.D., Powell, C.L., 2006. Methanogenic calcite, ^{13}C -depleted bivalve shells, and gas hydrate from a mud volcano offshore southern California. *Geology* 34 (2), 109.
- Holt, N.M., García-Veigas, J., Lowenstein, T.K., Giles, P.S., Williams-Stroud, S., 2014. The major-ion composition of Carboniferous seawater. *Geochim. Cosmochim. Acta* 134, 317–334.
- Horita, J., Zimmermann, H., Holland, H.D., 2002. Chemical evolution of seawater during the Phanerozoic. *Geochim. Cosmochim. Acta* 66 (21), 3733–3756.
- Ibach, L.E.J., 1982. Relationship between sedimentation rate and total organic carbon content in ancient marine sediments. *Am. Assoc. Pet. Geol. Bull.* 66 (2), 170–188.
- Immenhauser, A., Schöne, B.R., Hoffmann, R., Niedermayr, A., 2016. Mollusc and brachiopod skeletal hard parts: intricate archives of their marine environment. *Sedimentology* 63 (1), 1–59.
- Ivany, L.C., 2012. Reconstructing paleoseasonality from accretionary skeletal carbonates – challenges and opportunities. *Paleontol. Soc. Pap.* 18, 133–165.
- Jones, D.S., Quitmyer, I.R., 1996. Marking time with bivalve shells: oxygen isotopes and season of annual increment formation. *Palaios* 11 (4), 340.
- Jørgensen, B.B., Kasten, S., 2006. Sulfur cycling and methane oxidation. In: Schulz, H.D., Zabel, M. (Eds.), *Marine Geochemistry*, pp. 271–309.
- Kauffman, E.G., Arthur, M.A., Howe, B., Scholle, P.A., 1996. Widespread venting of methane-rich fluids in Late Cretaceous (Campanian) submarine springs (Tepee Buttes), Western Interior seaway, U.S.A. *Geology* 24 (9), 799–802.
- Kemp, D.B., Robinson, S.A., Crame, J.A., Francis, J.E., Ineson, J., Whittle, R.J., Bowman, V., O'Brien, C., 2014. A cool temperate climate on the Antarctic Peninsula through the latest Cretaceous to early Paleogene. *Geology* 42 (7), 583–586.
- Klein, R.T., Lohmann, K.C., Thayer, C.W., 1996. Sr/Ca and $^{13}\text{C}/^{12}\text{C}$ ratios in skeletal calcite of *Mytilus trossulus*: covariation with metabolic rate, salinity, and

- carbon isotopic composition of seawater. *Geochim. Cosmochim. Acta* 60 (21), 4207–4221.
- Knittel, K., Boetius, A., 2009. Anaerobic oxidation of methane: progress with an unknown process. *Annu. Rev. Microbiol.* 63, 311–334.
- Krantz, D.E., Williams, D.F., Jones, D.S., 1987. Ecological and paleoenvironmental information using stable isotope profiles from living and fossil molluscs. *Palaeogeogr. Palaeoclimatol. Palaeoecol.* 58 (3), 249–266.
- Kvenvolden, K.A., 1993. Gas hydrates—geological perspective and global change. *Rev. Geophys.* 31 (2), 173.
- Lartaud, F., de Rafelis, M., Oliver, G., Krylova, E., Dyment, J., Ildefonse, B., Thibaud, R., Gente, P., et al., 2010. Fossil clams from a serpentinite-hosted sedimented vent field near the active smoker complex Rainbow, MAR, 36°13'N: insight into the biogeography of vent fauna. *Geochem. Geophys. Geosyst.* 11 (8).
- Lawver, L.A., Gahagan, L.M., Coffin, M.F., 1992. The development of paleoseaways around Antarctica. In: Kennett, J.P., Warnke, D.A. (Eds.), *The Antarctic Paleoenvironment: a Perspective on Global Change*. In: *Antarct. Res. Ser.*, pp. 7–30.
- Little, C.T.S., Birgel, D., Boyce, A.J., Crame, J.A., Francis, J.E., Kiel, S., Peckmann, J., Pirrie, D., et al., 2015. Late Cretaceous (Maastrichtian) shallow water hydrocarbon seeps from Snow Hill and Seymour Islands, James Ross Basin, Antarctica. *Palaeogeogr. Palaeoclimatol. Palaeoecol.* 418, 213–228.
- Lowenstein, T.K., Hardie, L.A., Timofeeff, M.N., Demicco, R.V., 2003. Secular variation in seawater chemistry and the origin of calcium chloride basinal brines. *Geology* 31 (10), 857–860.
- Macellari, C.E., 1988. Stratigraphy, sedimentology, and paleoecology of Upper Cretaceous/Paleocene shelf-deltaic sediments of Seymour Island. In: *Mem. Geol. Soc. Amer.*, vol. 169, pp. 25–54.
- Martens, C., Blair, N., Green, C., Des Marais, D., 1986. Seasonal variations in the stable carbon isotopic signature of biogenic methane in a coastal sediment. *Science* 233 (4770), 1300–1303.
- McArthur, J.M., Thirlwall, M.F., Engkilde, M., Zinsmeister, W.J., Howarth, R.J., 1998. Strontium isotope profiles across K/T boundary sequences in Denmark and Antarctica. *Earth Planet. Sci. Lett.* 160 (1–2), 179–192.
- McConnaughey, T.A., Burdett, J., Whelan, J.F., Paull, C.K., 1997. Carbon isotopes in biological carbonates: respiration and photosynthesis. *Geochim. Cosmochim. Acta* 61 (3), 611–622.
- McConnaughey, T.A., Gillikin, D.P., 2008. Carbon isotopes in mollusk shell carbonates. *Geo Mar. Lett.* 28 (5–6), 287–299.
- Mook, W.G., Tan, F.C., 1991. Stable carbon isotopes in rivers and estuaries. In: *Biogeochemistry of Major World Rivers*, pp. 245–264.
- Owens, J.D., Gill, B.C., Jenkyns, H.C., Bates, S.M., Severmann, S., Kuypers, M.M.M., Wood, R.G., Lyons, T.W., 2013. Sulfur isotopes track the global extent and dynamics of euxinia during Cretaceous Oceanic Anoxic Event 2. *Proc. Natl. Acad. Sci. USA* 110 (46), 18407–18412.
- Paull, C.K., Martens, C.S., Chanton, J.P., Neumann, A.C., Coston, J., Jull, A.J.T., Toolin, L.J., 1989. Old carbon in living organisms and young CaCO₃ cements from abyssal brine seeps. *Nature* 342 (6246), 166–168.
- Petersen, S.V., Dutton, A., Lohmann, K.C., 2016. End-Cretaceous extinction in Antarctica linked to both Deccan volcanism and meteorite impact via climate change. *Nat. Commun.* 7, 12079.
- Poulain, C., Lorrain, A., Mas, R., Gillikin, D.P., Dehairs, F., Robert, R., Paulet, Y.-M., 2010. Experimental shift of diet and DIC stable carbon isotopes: influence on shell $\delta^{13}\text{C}$ values in the Manila clam *Ruditapes philippinarum*. *Chem. Geol.* 272 (1–4), 75–82.
- Prouty, N.G., Sahy, D., Ruppel, C.D., Roark, E.B., Condon, D., Brooke, S., Ross, S.W., Demopoulos, A.W.J., 2016. Insights into methane dynamics from analysis of authigenic carbonates and chemosynthetic mussels at newly-discovered Atlantic Margin seeps. *Earth Planet. Sci. Lett.* 449, 332–344.
- Reeburgh, W.S., 2007. Oceanic methane biogeochemistry. *Chem. Rev.* 107 (2), 486–513.
- Schoepfer, S.D., Tobin, T.S., Witts, J.D., Newton, R.J., 2017. Intermittent euxinia in the high-latitude James Ross Basin during the latest Cretaceous and earliest Paleocene. *Palaeogeogr. Palaeoclimatol. Palaeoecol.* 477, 40–54.
- Schöne, B.R., Fiebig, J., Pfeiffer, M., Gleß, R., Hickson, J., Johnson, A.L.A., Dreyer, W., Oschmann, W., 2005a. Climate records from a bivalved *Methuselah* (Arctica islandica, Mollusca; Iceland). *Palaeogeogr. Palaeoclimatol. Palaeoecol.* 228 (1–2), 130–148.
- Schöne, B.R., Houk, S.D., Freyre Castro, A.D., Fiebig, J., Oschmann, W., Kroncke, I., Dreyer, W., Gosselck, F., 2005b. Daily growth rates in shells of *Arctica islandica*: assessing sub-seasonal environmental controls on a long-lived bivalve mollusk. *Palaios* 20 (1), 78–92.
- Timofeeff, M.N., Lowenstein, T.K., da Silva, M.A.M., Harris, N.B., 2006. Secular variation in the major-ion chemistry of seawater: evidence from fluid inclusions in Cretaceous halites. *Geochim. Cosmochim. Acta* 70 (8), 1977–1994.
- Tobin, T.S., Ward, P.D., 2015. Carbon isotope ($\delta^{13}\text{C}$) differences between Late Cretaceous ammonites and benthic mollusks from Antarctica. *Palaeogeogr. Palaeoclimatol. Palaeoecol.* 428, 50–57.
- Tobin, T.S., Ward, P.D., Steig, E.J., Olivero, E.B., Hilburn, I.A., Mitchell, R.N., Diamond, M.R., Raub, T.D., et al., 2012. Extinction patterns, $\delta^{18}\text{O}$ trends, and magnetostratigraphy from a southern high-latitude Cretaceous–Paleogene section: links with Deccan volcanism. *Palaeogeogr. Palaeoclimatol. Palaeoecol.* 350, 180–188.
- Toland, H., Perkins, B., Pearce, N., Keenan, F., Leng, M.J., 2000. A study of sclerochronology by laser ablation ICP-MS. *J. Anal. At. Spectrom.* 15 (9), 1143–1148.
- Van der Nat, F.-J., Middelburg, J.J., 2000. Methane emission from tidal freshwater marshes. *Biogeochemistry* 49 (2), 103–121.
- Voigt, S., Gale, A.S., Jung, C., Jenkyns, H.C., 2012. Global correlation of Upper Campanian–Maastrichtian successions using carbon-isotope stratigraphy: development of a new Maastrichtian timescale. *Newsl. Stratigr.* 45 (1), 25–53.
- Wassmann, P., Svendsen, H., Keck, A., Reigstad, M., 1996. Selected aspects of the physical oceanography and particle fluxes in fjords of northern Norway. *J. Mar. Syst.* 8, 53–71.
- Whiticar, M.J., 1999. Carbon and hydrogen isotope systematics of bacterial formation and oxidation of methane. *Chem. Geol.* 161 (1–3), 291–314.
- Witts, J.D., Whittle, R.J., Wignall, P.B., Crame, J.A., Francis, J.E., Newton, R.J., Bowman, V.C., 2016. Macrofossil evidence for a rapid and severe Cretaceous–Paleogene mass extinction in Antarctica. *Nat. Commun.* 7, 11738.
- Witts, J.D., Newton, R.J., Mills, B.J.W., Wignall, P.B., Bottrell, S.H., Hall, J.L.O., Francis, J.E., Alistair Crame, J., 2018. The impact of the Cretaceous–Paleogene (K–Pg) mass extinction event on the global sulfur cycle: evidence from Seymour Island, Antarctica. *Geochim. Cosmochim. Acta* 230, 17–45.
- Wortmann, U.G., Chernyavsky, B.M., 2007. Effect of evaporite deposition on Early Cretaceous carbon and sulphur cycling. *Nature* 446, 654–656.
- Wortmann, U.G., Paytan, A., 2012. Rapid variability of seawater chemistry over the past 130 million years. *Science* 337 (6092), 334–336.
- Zachos, J.C., Pagani, M., Sloan, L., Thomas, E., Billups, K., 2001. Trends, rhythms, and aberrations in global climate 65 Ma to present. *Science* 292 (5517), 686–693.
- Zeikus, J.G., Winfrey, M.R., 1976. Temperature limitations of methanogenesis in aquatic sediments. *Appl. Environ. Microbiol.* 31 (1), 99–107.
- Zhang, G., Zhang, J., Liu, S., Ren, J., Xu, J., Zhang, F., 2008. Methane in the Changjiang (Yangtze River) Estuary and its adjacent marine area: riverine input, sediment release and atmospheric fluxes. *Biogeochemistry* 91 (1), 71–84.
- Zinsmeister, W.J., 1998. Discovery of fish mortality horizon at the K–T boundary on Seymour Island: re-evaluation of events at the end of the Cretaceous. *J. Paleontol.* 72 (03), 556–571.